ELSEVIER

Polymer 42 (2001) 6141–6152

polymer

www.elsevier.nl/locate/polymer

Late stages of ordering of thin polymer films on chemically heterogeneous substrates: energetics and metastability

Z. Shou, A. Chakrabarti*

Department of Physics, Kansas State University, 116 Cardwell Hall, Manhattan, KS 66506-2601, USA

Received 2 October 2000; received in revised form 28 December 2000; accepted 2 January 2001

Abstract

By a direct numerical integration of the dynamical evolution equations, we study phase separation of thin polymer blend films in two-dimensional models. The focus of our work is on the late-time morphology of the films. We first investigate morphological transitions in a thin film on a flat, homogeneous substrate. In particular, we probe the transition between a completely wetting and a partially wetting surface morphology. This transition is controlled by a competition between surface interactions and the interfacial energy in a thin film. This competition becomes even more pronounced when a chemically patterned substrate is used. For films cast on a patterned substrate, we consider several different substrate pattern widths and surface interaction strengths in our simulations. We also probe effects of thermal fluctuations on the late-time film morphology by carrying out simulations to many different final quench temperatures. Along with quench simulations, we further study film morphology by slow cooling the film from an initial high temperature. Comparing the morphology of films for a quench case to a slow-cooling case, we identify possible barriers to reaching equilibrium in experimental situations under a quench.

Keywords: Thin polymer films; Thermal fluctuations; Slow cooling

1. Introduction

Polymeric thin films on solid substrates have important applications in protective coatings, lubrication, adhesives, and micro-electronics. Experimental techniques have recently been developed to create surfaces patterned with imprinted structures which can be used to guide structure formation in thin films of polymer mixtures [1,2] and block copolymers (BCP) [3,4]. A major interest in these studies is to control the morphology of these thin films by carefully choosing external parameters such as type of substrates and film thickness. Control of film morphology may lead to important applications in diverse fields [5,6] such as opto-electronic devices and templating in lithographic processes.

The presence of a surface alters the course of phase separation in a bulk polymer blend by breaking translational and rotational symmetry. It has been found experimentally [7,8] that preferential attraction of one of the components of a polymer blend to a laterally homogeneous surface causes a spinodal wave to grow with a dominant wave-vector directed normal to the surface. Wetting effects affect the kinetics of phase separation near the surface and this results in a fast growth of domains near the surface [9,10]. Recent experiments [1,2] show that domains of a phase separating thin film of a polymer mixture of critical composition can be guided into arbitrary structures in the presence of a chemically inhomogeneous substrate with pre-patterned surface energy variation.

To understand the intrinsic thermodynamic nature of these phenomena, different theoretical and numerical models and schemes have recently been applied to the study of phase separation of polymer blends cast on chemically patterned surfaces. Seok, Freed and Szleifer have employed [11] an analytical density-functional theory to study composition variations in the single-phase region of a compressible polymer blend near a chemically patterned surface. They found that the near-surface profiles are primarily determined by the competition of several length scales and relevant physical parameters while the strength of surface interaction mainly controls the magnitude of surface segregation. Phase separation of thin polymer blend films on a chemically heterogeneous surface has recently been investigated numerically by two groups. Karim et al. [2] have supplemented their experimental work of atomic force microscopy by carrying out simulations in two-dimensions. They have found that phase separation in thin films follows the underlying pattern of the substrate while in thicker films

---

* Corresponding author. Tel.: +1-785-532-6786; fax: +1-785-532-6806.
E-mail address: amitc@phys.ksu.edu (A. Chakrabarti).

0032-3861/01/$ - see front matter © 2001 Published by Elsevier Science Ltd.
PII: S0032-3861(01)00054-4

the existence of a 'checkerboard' pattern was observed. More recently, Kielhorn and Muthukumar [12] have carried out simulations in three dimensions to study the effects of a patterned surface on the kinetics of phase separation in thin polymer blend films. Although this simulation is mostly limited to deep quenches (weak noise strengths), interesting effects of the patterned surface on the kinetics of phase separation are observed in this work. For example, they find a transient out-of-phase stripe pattern for thin films at the top layer (experimentally this will be the air/polymer interface) of the film and the existence of a composition wave associated with a checkerboard-like pattern formation. They also find that surface-induced fluctuations can dissolve for weak surface interactions and bulk phase separation dominates the phase separation kinetics in such situations.

In this paper, we concentrate primarily on the late-time morphology of polymer blend films on patterned surfaces. The focus of our work is distinctly different from previous numerical work of Karim et al. and Kielhorn and Muthukumar. First, we probe the effects of thermal fluctuations on the late-time morphology by carrying out simulations for many different final quench temperatures. This aspect of the numerical calculations was absent in previous studies where mostly deep quenches (weak noise strengths) were considered. Next, we consider several different substrate pattern widths and surface interaction strengths so that the late-time morphology of the film can either be dominated by surface interactions or by the interfacial energy. Along with quench simulations we also study film morphology at the final temperature by slow cooling (simulated annealing) the system from an initial high temperature single phase. This procedure allows the system to reach an equilibrium configuration for that particular final temperature. Comparing the morphology of the films at late times after a quench with the morphology of the same film under a slow-cooling procedure, we look for long-lived metastable states associated with a low-temperature quench. This allows us to identify whether there are possible barriers to reaching equilibrium in experimental situations under a quench. This aspect of our simulations is quite important and relevant for experimentally controlling film morphology by using a surface motif.

Results presented in this paper are obtained from a numerical study of a Cahn–Hilliard type coarse-grained model (for a review see Ref. [13]) of polymer thin films confined between two hard walls, one being neutral to the components of the blend and the other one containing chemical in-homogeneities with a repeat spacing length scale which is varied in the simulations. For homogeneous substrates, we previously carried out calculations for both short-range [14] and long-range [15] surface interactions using this model. For a critical composition of the blend, we previously found that the thickness of the surface layer increases with time as $t^{1/3}$ before the surface saturates. In a previous paper, we also calculated the density profile as a function of distance from the surface for various times after the quench. The density profile shows damped oscillations similar to those obtained in experiments. A scaling description of these density profiles is possible as the thickness of the layer turns out to be the only relevant length scale near the surface. Thus, if one rescaled distance from the surface by the wetting-layer thickness, one expects to obtain a time-independent single master curve for the density profiles. The $t^{1/3}$ growth law and the scaling of the density profile have been verified in experimental studies [8] with polymer blends. As well, model calculations of density profiles for off-critical quenches [14] and interference of spinodal waves [16] in thin film geometry are also in good agreement with experimental observations. The success of the model for laterally homogeneous surfaces suggests that it is well suited for our proposed studies with patterned surfaces.

Pattern formation in thin films on a chemically heterogeneous substrate may depend on a wide variety of parameters of the system. These would include the detailed characteristics of the substrate such as the strength and range of the surface interactions, the length scale of the surface inhomogeneities, and the film thickness, in addition to the usual parameters characterizing the blend such as the interfacial energy between the two components and temperature. In order to probe late-time morphology of the film for a large set of parameters, we restrict our simulations to two-dimensions. For this reason, the results cannot be directly compared with experimental results. Moreover, the top surface in our simulations is rigid and has no preferential enrichment while in experimental situations the films have a free and deformable polymer–air boundary that preferentially enriches one of the blend components. In addition, the absence of hydrodynamic interactions is a further shortcoming of the theoretical model considered here. However, the main findings of the simulations such as the effects on the film morphology due to (i) a competition between surface energy and interfacial energy, (ii) thermal fluctuations, and (iii) the presence of possible barriers to reach final equilibrium state after a quench are still important and relevant for laboratory experiments.

The rest of the paper is organized as follows. In Section 2, we briefly describe the model and the numerical methods used in the study. In Section 3, we present our main results and describe how the competition between surface interactions and the interfacial energy dictates the late-time morphology of thin films at various temperature of quench. We conclude in Section 4 with a summary of our results and a discussion of the relevance of these results in experimental situations.

2. Model and numerical procedure

In the phenomenological approach used in this paper, the concentration filed, $\phi(\vec{r}, t)$, is chosen to be the local concentration difference between the two components of the blend, and the free energy functional (in units of $k_B T$) for the bulk system is considered to have a Ginzburg–Landau form:

$$F_{\mathrm{bulk}}[\phi(\vec{r},t)] = \int \mathrm{d}\vec{r}\left[-\frac{b}{2}\phi^2 + \frac{u}{4}\phi^4 + \frac{K}{2}|\nabla\phi|^2\right], \tag{1}$$

where b, u, and K are parameters of the model. The dynamical evolution after a quench from a high-temperature disordered state to a final temperature much below the critical temperature is modeled by the Cahn–Hilliard type equation:

$$\frac{\partial\phi}{\partial t} = M\nabla^2\mu + \eta, \tag{2}$$

where M is the mobility (assumed a constant here), $\mu = \delta F/\delta\phi$ the local chemical potential, and η the thermal noise. After a suitable rescaling of the concentration field, time, and space, the above equation can be written in a simple dimensionless form:

$$\frac{\partial\phi}{\partial t} = \nabla^2(-\phi + \phi^3 - \nabla^2\phi) + \sqrt{\varepsilon}\eta \tag{3}$$

which is the basic dynamical equation of the model for the bulk system. Here, $\sqrt{\varepsilon}$ is the strength of the noise term and is proportional to the final temperature of quench. The thermal noise η satisfies the following fluctuation–dissipation relation:

$$\langle\eta(\vec{r},t)\eta(\vec{r}',t')\rangle = -\nabla^2\delta(\vec{r}-\vec{r}')\delta(t-t'). \tag{4}$$

In this paper, we consider a $L \times L_z$ thin film system. This thin film system is confined between two rigid surfaces at a distance $L_z - 1$ apart. The surface at $z = 0$ is a chemically heterogeneous substrate, while the surface at $z = L_z - 1$ is a neutral one. The chemically heterogeneous substrate is patterned as strips of the same width w. They are alternatively attractive to the A and B components of the blend. This interaction is incorporated by including a contact potential in the free-energy functional. The complete free-energy functional is:

$$F[\phi] = F_{\mathrm{bulk}}[\phi] - \int \mathrm{d}\vec{r}[\sigma(x)\delta(z)]\phi(x,z,t), \tag{5}$$

where $\sigma(x)$ is the contact potential given by:

$$\sigma(x) = \left\{\begin{array}{ll} \sigma_0 & 2nw \le x < (2n+1)w, \\ -\sigma_0 & (2n+1)w \le x < 2(n+1)w, \end{array}\right\} \tag{6}$$

and $n = 0, 1, \ldots, L/2w - 1$. The surface energy model considered here does not incorporate the boundary interaction associated with the change of the polymer–polymer interaction at the boundary. This surface interaction parameter does not seem to affect the qualitative physics over the parameter range considered [19]. In the presence of hard surfaces, the global conservation of concentration is satisfied by including a boundary condition that does not allow mass transport perpendicular to the walls. These boundary conditions at the surfaces $z = 0$ and $z = L_z - 1$ are:

$$\hat{\mathbf{z}}\cdot\nabla\phi(\mathbf{r},t)|_{\mathrm{surface}} = 0 \tag{7}$$

$$\hat{\mathbf{z}}\cdot\nabla\mu(\mathbf{r},t)|_{\mathrm{surface}} = 0 \tag{8}$$

We use a periodic boundary condition in the lateral direction (x-direction).

We have simulated Euler-discretized version of the evolution equations with boundary conditions (7) and (8) on two-dimensional systems of size $L \times L_z$. Two different cooling methods were used in the simulations. In the first method, we quench the system from a high temperature phase to the final temperature governed by ε. In this case, the thermal noise strength ε is set to a fixed value right from the beginning ($t = 0$). In the slow cooling or simulated annealing method, we gradually equilibrate the system by evenly decreasing the noise strength from a high value $\varepsilon_{\max}$ to the target value ε. Normally, we divide the range $\varepsilon_{\max}-\varepsilon$ into ten steps, and at each step, we anneal the system for about 240,000 time steps with $\Delta t = 0.01$.

In order to quantitatively measure the amount of domain line-up (or overlap) with the pre-assigned chemical structure of the substrate as a function of time t and the distance z from the substrate, we introduce a quantity $p(z,t)$ defined as

$$p(z,t) = \frac{1}{L}\sum_x (2\Theta(\sigma(x)\phi(x,z,t) - 1) \tag{9}$$

where the $\Theta(\cdot)$ is the Heaviside step function, defined as:

$$\Theta(x) = \left\{\begin{array}{ll} 1 & \text{for } x \ge 0, \\ 0 & \text{for } x < 0. \end{array}\right\} \tag{10}$$

A similar overlap function was first introduced by Chen and Chakrabarti [17,18] for studying ordering of block copolymer thin films on patterned substrates and has recently been used by Kielhorn and Muthukumar [12] in their study of polymer thin films. The late-time value of the overlap will loosely be called $p_{\mathrm{eq}}(z)$: this is computed at a very late time after a quench when the system does not seem to evolve further and also by a simulated annealing method where the system reaches an equilibrium configuration.

3. Results

3.1. Plating-droplet transition in a thin film

Before proceeding to the numerical simulation of phase separation of polymer thin films on a patterned substrate, we first investigate morphological transitions in a thin film on a flat, homogeneous substrate. In particular, we probe the transition between a completely wetting surface morphology (called “plating”) to a partially wetting morphology of surface droplets. This transition has been well studied by Marko [19] for *bulk* systems. Our focus here is to study how this transition is affected when the thickness of the film is reduced. This sets the stage for a competition between surface interactions and the interfacial energy in a thin film, which will be even more pronounced when a chemically patterned substrate is used. For comparison, we

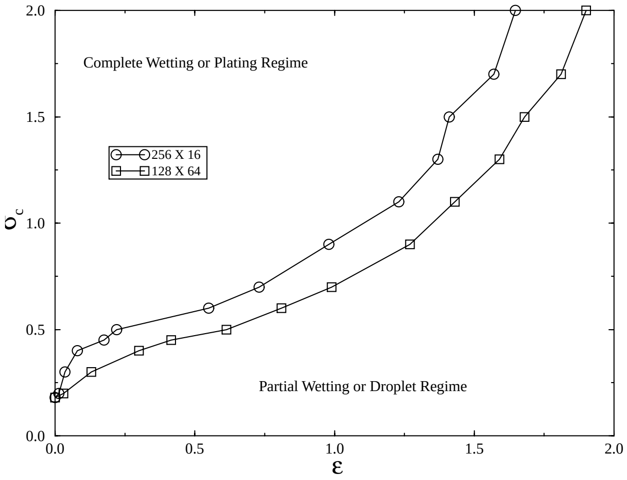

Fig. 1. Morphology diagram of plating (complete wetting) to droplet (partial wetting) transition in systems of two different sizes.

compute plating-droplet morphology diagrams for systems of size 256×16 and 128×64. For each homogeneous surface potential considered, we vary the final thermal noise strength ε and determine the plating-droplet transition. In each case the system is slow cooled from a high temperature, random initial condition to the final temperature (or ε) for 2,400,000 time steps. This procedure irons out defects in the system and the film reaches an equilibrium configuration for the final value of the ε. To determine the plating to droplet transition in a quantitative fashion, we define the following laterally-averaged composition profile after a slow cooling:

$$\rho(z) = \frac{1}{L} \sum_x \phi(x, z). \tag{11}$$

When $\rho(0) \geq 0.99$, the film morphology is considered to be in a plating phase, i.e., the substrate is 'completely' wetted by the preferred component. Otherwise, it is considered to be in a surface droplet phase, where there are considerable number of sites on the substrate occupied by the unfavored component of the blend. Fig. 1 shows the plating-droplet transition morphology diagram for the two system sizes considered in this study. The critical value of the surface interaction strength for this transition (σ_c) increases with thermal noise strength in each case. It is interesting to note that σ_c is higher for the thinner film for the same value of ε. For a fixed temperature, then, one needs a stronger surface potential for a thin film to be a in a plating morphology. This trend in the morphology diagram as the thickness of the film is reduced can be understood by a simple argument. For a completely phase separated final state at a low temperature, we consider two types of domain morphology: a plating morphology with phase separated domains parallel to the substrate, and a 'droplet' morphology with phase separated domains being perpendicular to the substrate. From a simple calculation of interfacial energy contributions and surface energy contributions to the free-energy of the film in these two configurations, we conclude that the plating morphology will be favorable in a two-dimensional system when

$$\sigma > \gamma\left(1 - \frac{L_z}{L}\right), \tag{12}$$

where γ is the interfacial tension between the two components of the blend. For the first system of size 256×16, $L_z/L = 1/16$, while for the second system of size 128×64, $L_z/L = 1/4$. Thus the critical value of σ for the first system needs to be larger for the same value of temperature. This confirms the trend observed in the simulation. A similar trend should exist for three-dimensional systems as well.

3.2. Patterned substrates with narrow strips

Domain growth in a thin film cast on a patterned substrate is also controlled by the competition between the interfacial energy of the two components of the blend and the surface energy provided by the substrate. The interfacial tension γ in a *deep quench* can be obtained by assuming a mean-field concentration profile:

$$\phi(z) = \phi_0 \tanh\left(\frac{z}{\sqrt{2}\xi}\right) \tag{13}$$

where ϕ_0 is the equilibrium value of the concentration deep inside the domains, and ξ the correlation length (thickness of the interface). This would yield [13]

$$\gamma = \frac{2\sqrt{2}}{3} \frac{\phi_0^2}{\xi} \tag{14}$$

Since in a deep quench situation, $\phi_0 \approx 1$, and $\xi \approx 1$ in our model, $\gamma \approx 0.94$ from Eq. (14). This estimate for γ should only work for deep quenches; at other quench temperatures the value of γ should be *lower* than this estimate.

In order to estimate whether the pattern formation in a thin film is controlled by the surface energy or by the interfacial energy, we need to compare the surface potential per strip $w\sigma_0$ with the interfacial energy per strip $L_z\gamma$. If $w\sigma_0 \gg L_z\gamma$, surface interaction dominates over the interfacial tension. In such a situation, lateral growth of domains will be restricted in the thin film as this growth is manifested by reducing the interfacial tension. Consequently, each component of the blend would be 'pinned' to the preferred strips to minimize the total surface energy. The late-time patterns will then be regularly ordered following the substrate motif and the overlap with the underlying surface pattern will be very large. In contrast, if $w\sigma_0 \ll L_z\gamma$, interfacial energy would be the dominant term in the total free energy and domains would grow laterally crossing the boundaries set by the surface patterns. In such a situation, bulk like phase separation would take place and the overlap with the underlying surface pattern will be small, particularly when one moves away from the substrate (i.e. with increasing z).

For the results presented in this section, the surface strip width w is eight units and the system size is 256×16. Although we have considered several values of the surface interaction strength σ_0 in the simulation, we will concentrate here on two particular cases: (i) $\sigma_0 = 0.3$; and (ii) $\sigma_0 = 2.2$. In case (i), interfacial energy dominates the pattern formation while in case (ii) the surface energy term has a slightly larger contribution toward the overall free-energy of the system.

In Fig. 2a and b we show the temporal evolution of the system in case (i) ($\sigma_0 = 0.3$) for two different quench temperatures $\varepsilon = 0.01$, and 0.6, respectively. At early times, phase separation starts out isotropically away from the substrate, while near the bottom layer, the striped substrate is quickly wetted by the respective preferred components. When the thermal fluctuations are weak (Fig. 2a), these wetting layers keep growing to form a preferred component enrichment layer which is followed by a depletion layer of the preferred component along the z-direction. Formation of the depletion layer right above the wetting layer is well known in the context of surface-directed spinodal decomposition. In the present case with a patterned substrate, this leads to a checkerboard-like pattern formation at early times as observed in previous experiments and simulations. Such a pattern formation leads to a damped oscillatory profile to the

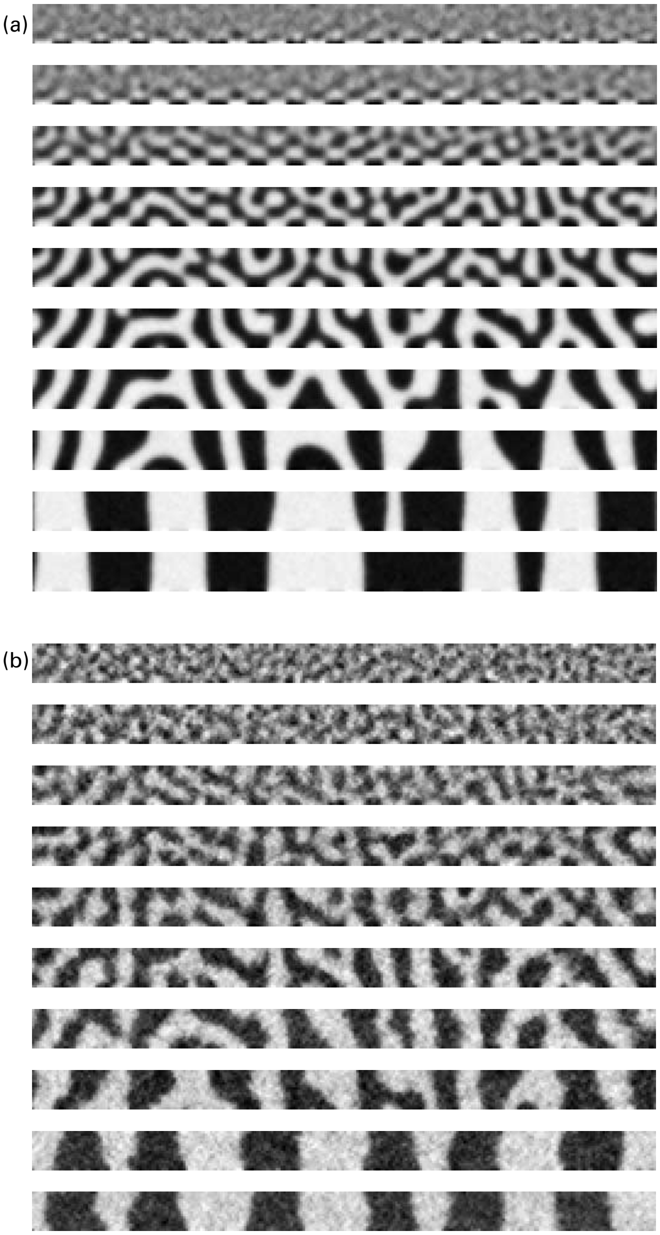

Fig. 2. Snapshots during the evolution of a thin film cast on a chemically patterned substrate under a temperature quench to two different final temperatures. In each case, the time sequence from top to bottom is $t = 3, 6, 12, 24, 48, 96, 192, 768, 10{,}800, 24{,}000$. The width of the surface pattern ($\omega = 8$) and the surface interaction strength ($\sigma = 0.3$) are the same in each case. In (a) the noise strength $\varepsilon = 0.01$ while in (b) it is given by $\varepsilon = 0.6$.

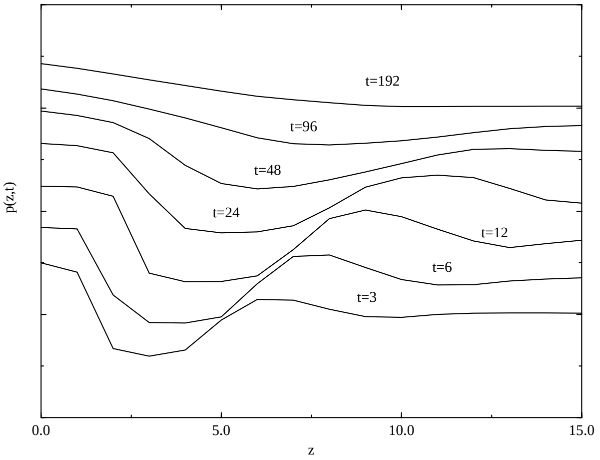

Fig. 3. Results for the overlap function $p(z, t)$ defined in Eq. (9), versus distance z from the substrate surface at various times. Here the width of the surface pattern is $\omega = 8$, surface interaction strength is $\sigma = 0.3$, and the strength of the thermal noise is $\varepsilon = 0.01$. Graphs for successive times are offset by an equal amount to maintain clarity.

time-dependent overlap function $p(z, t)$ as shown in Fig. 3. This type of oscillatory density profile has been observed in surface-directed spinodal decomposition. In the presence of a patterned substrate it is necessary to consider the overlap function rather than the density to capture this oscillatory profile. These well-defined checkerboard patterns observed at early times, are somewhat washed out when the thermal fluctuations are large (Fig. 2b).

As time progresses, domains in the lateral direction grow to minimize the interfacial energy between the two components of the blend. As noted earlier, the strength of the surface interaction is weak in this case and thus the late-time pattern formation should be controlled by the phase separation between the two components. This is observed in both Fig. 2a and b at late times. The late-time patterns cover more than one substrate strips. This would indicate that the overlap of the film morphology with the substrate pattern will be small in this case.

Next, we increase the surface interaction strength to $\sigma_0 = 2.2$. In this case, the net surface interaction has a larger contribution to the free-energy, although the condition $w\sigma_0 \gg L_z\gamma$ does *not* hold. For this condition to be satisfied here one would need such a large value of σ_0 that a numerical instability takes place in the simulation. In Fig. 4a and b we show the temporal evolution of the system in this case for two different quench temperatures $\varepsilon = 0.01$, and 0.6, respectively. As before, a prominent checkerboard-like pattern forms at early times particularly for low-temperature quenches. More interesting though are the late-time patterns in the system. The contribution of the surface energy is larger in this case compared to the interfacial energy term. One would expect then that the late-time morphology of the system would be ordered following the underlying surface patterns. This is certainly true very close to the substrate. A strong surface interaction readily holds the respective preferred components right onto the substrate patterns. But as the surface interaction is short-ranged and the interfacial energy contribution is still quite large for this choice of parameters, a lateral phase separation takes place on a size much larger than the size of the substrate strips right away from the substrate layer. Thus, even slightly away from the substrate, domain morphology covers many strips by crossing the boundaries set by the substrate patterns. This phenomenon has important ramifications in experimental situations. If the substrate pattern widths are small enough such that the interfacial energy will have a reasonably large contribution to the overall free-energy of the film, a well-aligned film morphology will be extremely difficult to attain even for strong surface interactions.

We now present results for the overlap $p_{\mathrm{eq}}(z)$ of the film morphology with the substrate pattern at late times. For a quench simulation, this quantity is computed at $t = 24,000$ when the concentration profile does not change further. In order to check whether the late-time morphology of the film is complicated by the presence of long-lived metastable states after a quench, we have compared our results for the overlap with slow cooling (simulated annealing) runs. These results are presented in Fig. 5a and b for $\sigma_0 = 0.3$ and $\sigma_0 = 2.2$, respectively. In Fig. 5a results for the quench simulations and the slow-cooling simulations are comparable to each other when the strength of the noise is moderately large. In these cases, the late-time conformation of the quenched film is very close to the true, equilibrium situation. The overlap remains small throughout the film as the energetics is dominated by the interfacial tension between the two components of the blend which results in domains of lateral size larger than the width of the surface patterns. For a deep quench with $\varepsilon = 0.05$ an interesting distinction appears between the quench case and the slow cooling case. The amount of overlap throughout the film is much larger for the quench case. As mentioned earlier, one expects that the energetics should be controlled by the interfacial tension for these choice of parameters leading to a *small* overlap with the substrate pattern. Thus, the relatively large overlap observed for the quench case must arise from a pinning of the domains near the substrate. This pinning which takes place at early times (which leads to the checkerboard pattern discussed earlier) is slowly released by lateral diffusion at higher temperatures. However, diffusion is suppressed at low temperatures and the pinning of domains by the substrate can survive for an enormously long time after a quench. In a simulated annealing procedure, however, the system is slow cooled from a high temperature and the metastability arising from the pinning is washed away by large thermal fluctuations available at high temperatures. Thus, metastable pinning effects can enhance alignment of the film to the substrate pattern in a deep quench situation. Washing out of pattern due to thermal fluctuations and at long times is also observed by Lee, Douglas and Glotzer in the case of filler particles in a polymer blend [20].

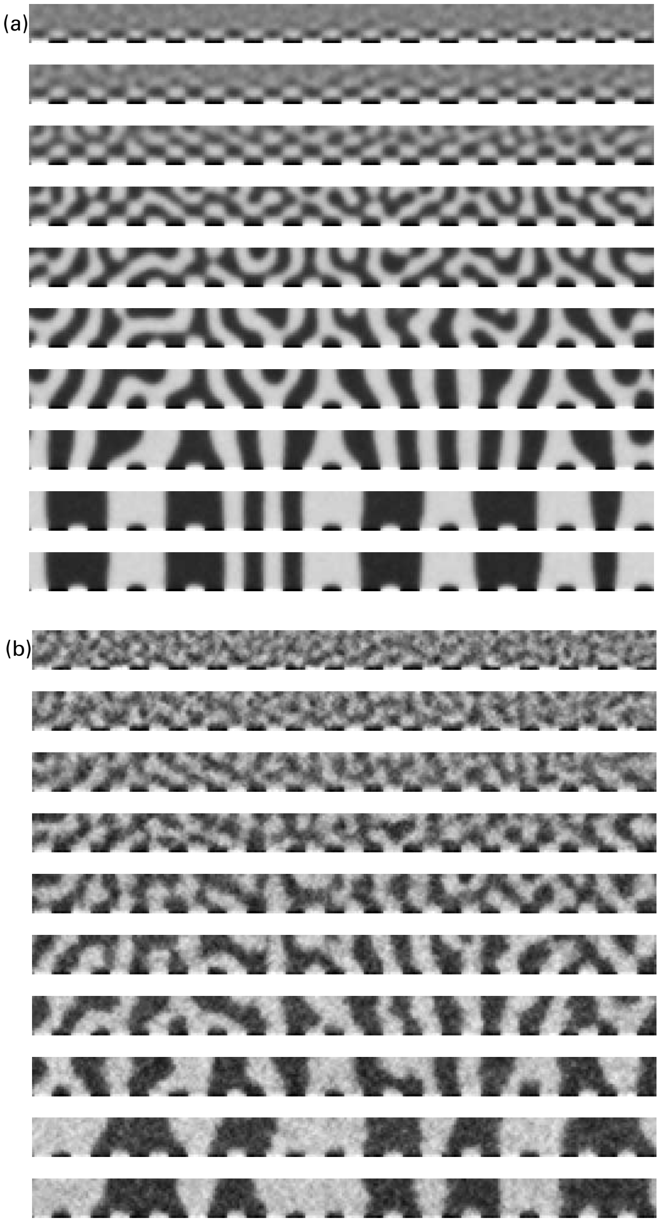

Fig. 4. Snapshots during the evolution of a thin film cast on a chemically patterned substrate under a temperature quench to two different final temperatures. In each case, the time sequence from top to bottom is $t = 3$, 6, 12, 24, 48, 96, 192, 768, 10,800, 24,000. The width of the surface pattern ($\omega = 8$) and the surface interaction strength ($\sigma = 2.2$) are the same in each case. In (a) the noise strength $\varepsilon = 0.01$ while in (b) it is given by $\varepsilon = 0.6$.

When the surface interaction is strong as in the cases of Fig. 5b, the film is perfectly aligned near the substrate at all temperatures considered here but the magnitude of this ordering decays as one moves away from the substrate. Phase separation of the two components driven by the interfacial energy dominates film morphology away from the substrate and domains spanning several substrate pattern widths form. As seen before, for larger values of the noise strength the quench results and slow-cooling results agree well with each other throughout the film. But for a low-temperature quench, the overlap in the film away from the substrate is larger than that computed in a slow-cooling case. The reason for this is similar to what we have just discussed in the preceding paragraph. The pinning introduced by a strong surface interaction survives for a long time in a deep quench as lateral diffusion is suppressed at a low temperature.

3.3. Patterned substrates with wide strips

Now we turn our attention to cases where the substrate strip widths are large. If the surface interactions are strong as well, one would possibly be able to probe film morphologies dominated by the substrate pattern, i.e. cases where $\sigma_0\omega$ is much larger than γL_z.

In Figs. 6 and 7 we show temporal evolution of systems

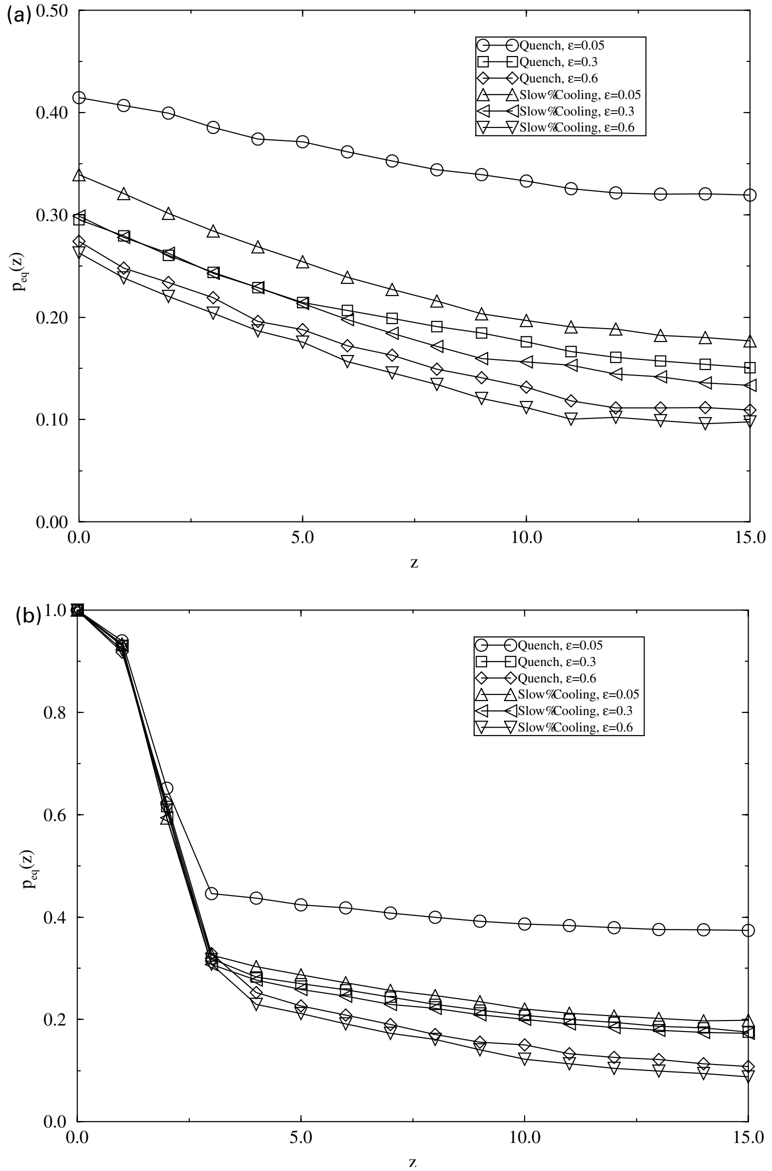

Fig. 5. The late-time domain overlap function after a quench is compared with the equilibrium domain overlap function obtained after a slow cooling of the system. In each case, the width of the surface pattern is $\omega = 8$. In (a) the strength of the surface interaction is $\sigma = 0.3$, while in (b) it is given by $\sigma = 2.2$.

with wide substrate pattern strips. In Fig. 6 $\omega = 18$ and $\sigma_0 = 0.3$ while in Fig. 7 $\omega = 24$ and $\sigma_0 = 1.0$. For Fig. 6 $\sigma_0\omega = 5.4$ while $\gamma L_z = 14.1$ (at least for deep quenches where our estimate for γ would be reasonably accurate). Although the contribution of the substrate potential is larger in this case when compared to the narrow width cases considered in previous sections, one would still expect that the film morphology be substantially influenced by the interfacial tension. For results shown in Fig. 7, however, $\sigma_0\omega = 24$ while γL_z is still 14.1. In these cases, the film morphology may be controlled by the substrate potential.

Let us now look closely at the film morphologies presented in Fig. 6a and b. In each of these cases, one observes the presence of a checkerboard pattern at early times. Such a pattern formation leads to a damped oscillatory profile for the time-dependent overlap function $p(z, t)$ similar to what has been presented in Fig. 3. The late-time behaviors for these two quenches are quite different though. For the low-noise case ($\varepsilon = 0.01$ in Fig. 6a) the final stages of the film morphology seem to largely follow the substrate pattern although a perfect match with the substrate pattern is not observed. This is because the contribution of the interfacial energy is still large in this case and this prevents the formation of a large number of interfaces. When the quench temperature is increased to $\varepsilon = 0.6$ in Fig. 6b, a much better match between the film morphology and the substrate pattern is observed at the final stages of the evolution process. This enhanced overlap takes place due to two reasons. First, at the higher quench temperature the value of γ is smaller than our estimate for deep quenches which reduces the interfacial energy cost for the additional number of interfaces between the two components. Also, a higher temperature of quench leads to increased diffusion of molecules which allows the system to properly find lowest energy states without being trapped in any metastable configuration. We will elaborate on this second point shortly.

When the strip width size ω and the surface interaction strength σ_0 are both increased in Fig. 7, surface energy contribution becomes much larger than the interfacial energy contribution. Even then, the final stages of the film morphology for the low-noise case ($\varepsilon = 0.01$ in Fig. 7a) does not yield a perfect match between the overall film morphology and the underlying substrate pattern. The substrate strips are wetted by the respective preferred components but away from the substrate this order melts occasionally. When a larger value for the final quench temperature is chosen in Fig. 7b ($\varepsilon = 0.6$) an almost perfect match between the film morphology and the substrate pattern is observed at the final stages of the evolution process. As before, this enhanced ordering is due to a reduction of the interfacial tension at higher temperatures and the ability of the system to avoid metastable configurations at higher temperatures.

Results for the overlap of the film morphology with the substrate pattern are presented in Fig. 8. As before, this quantity is computed at $t = 24,000$ for a quench simulation when the concentration profile does not change further. The

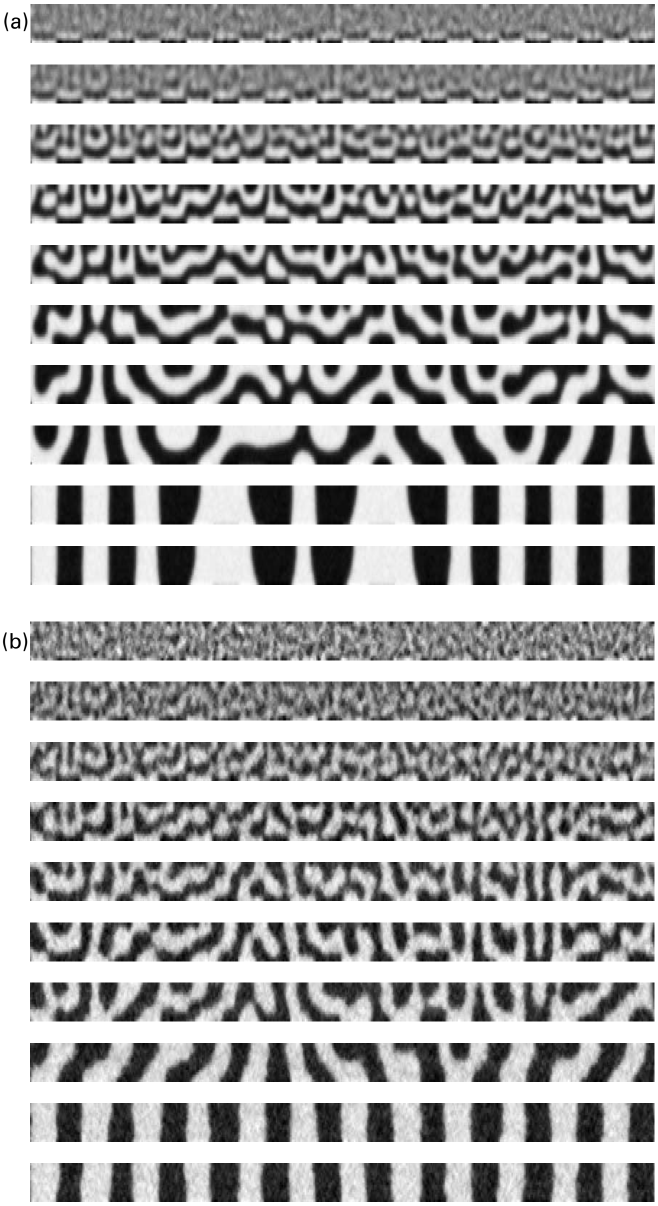

Fig. 6. Snapshots during the evolution of a thin film cast on a chemically patterned substrate under a temperature quench to two different final temperatures. In each case, the time sequence from top to bottom is $t = 3, 6, 12, 24, 48, 96, 192, 768, 10{,}800, 24{,}000$. The width of the surface pattern ($\omega = 18$) and the surface interaction strength ($\sigma = 0.3$) are the same in each case. In (a) the noise strength $\varepsilon = 0.01$ while in (b) it is given by $\varepsilon = 0.6$.

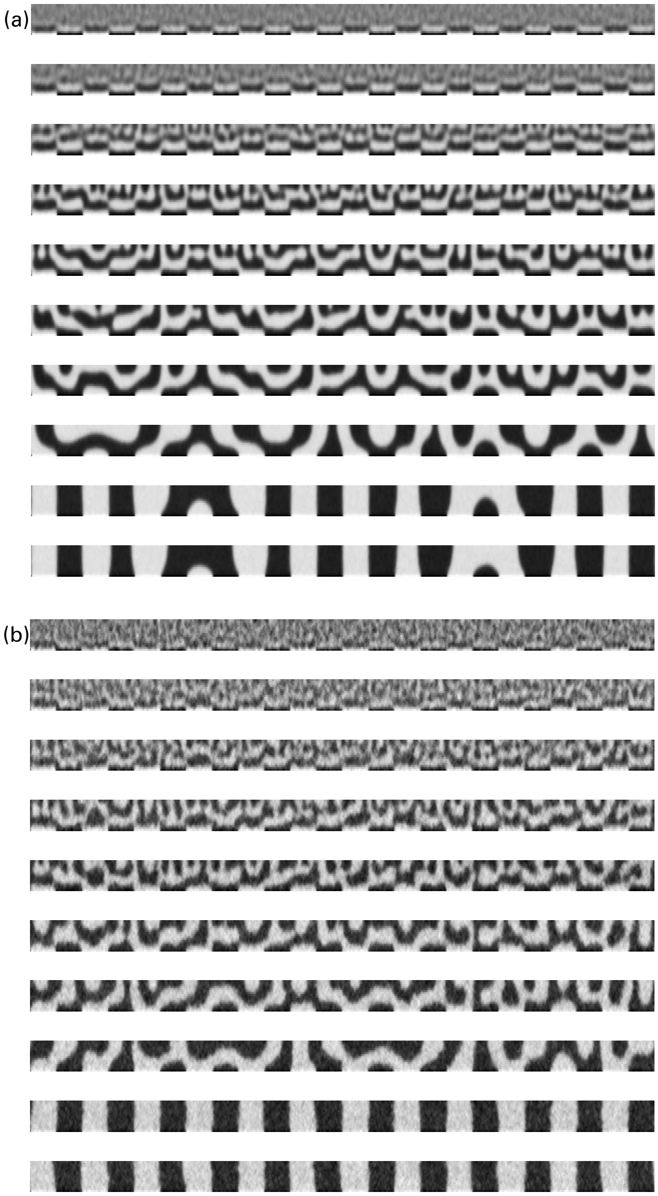

Fig. 7. Snapshots during the evolution of a thin film cast on a chemically patterned substrate under a temperature quench to two different final temperatures. In each case, the time sequence from top to bottom is $t = 3, 6, 12, 24, 48, 96, 192, 768, 10{,}800, 24{,}000$. The width of the surface pattern ($\omega = 24$) and the surface interaction strength ($\sigma = 1$) are the same in each case. In (a) the noise strength $\varepsilon = 0.01$ while in (b) it is given by $\varepsilon = 0.6$.

overlap is also computed when the system is slow cooled to the final temperature from a high, initial temperature. Results presented in Fig. 8a correspond to $\omega = 18$ and $\sigma_0 = 0.3$ while those in Fig. 8b are for $\omega = 24$ and $\sigma_0 = 1$. Note that for a low temperature quench with $\varepsilon = 0.05$ the overlap with the substrate pattern is larger throughout the film for a slow-cooling case. The trend between these two runs is totally different from the one observed for narrow width cases where slow cooling yields a *smaller* overlap with the substrate pattern. The difference between the slow-cooling case and the quench case is smaller (and actually negligible for $\varepsilon \geq 0.45$) as the temperature of quench is increased. We have already noted in Fig. 6a that the matching between the film morphology and the substrate pattern improves as the quench temperature is increased. Fig. 8a describes this in a quantitative fashion. The discrepancy between slow-cooling results and quench results at low temperatures arises for the following reason. Since the substrate interaction is short ranged, the blend away from the substrate does not feel this and starts to phase separate in the usual, bulk like fashion at early times. Diffusion of molecules would align the film toward the surface pattern at late times. But such diffusion is suppressed at low temperatures of quench and thus the film would take a prohibitively long time to reach an ordered state. In a slow-cooling run though, the system spends enough time at higher temperatures

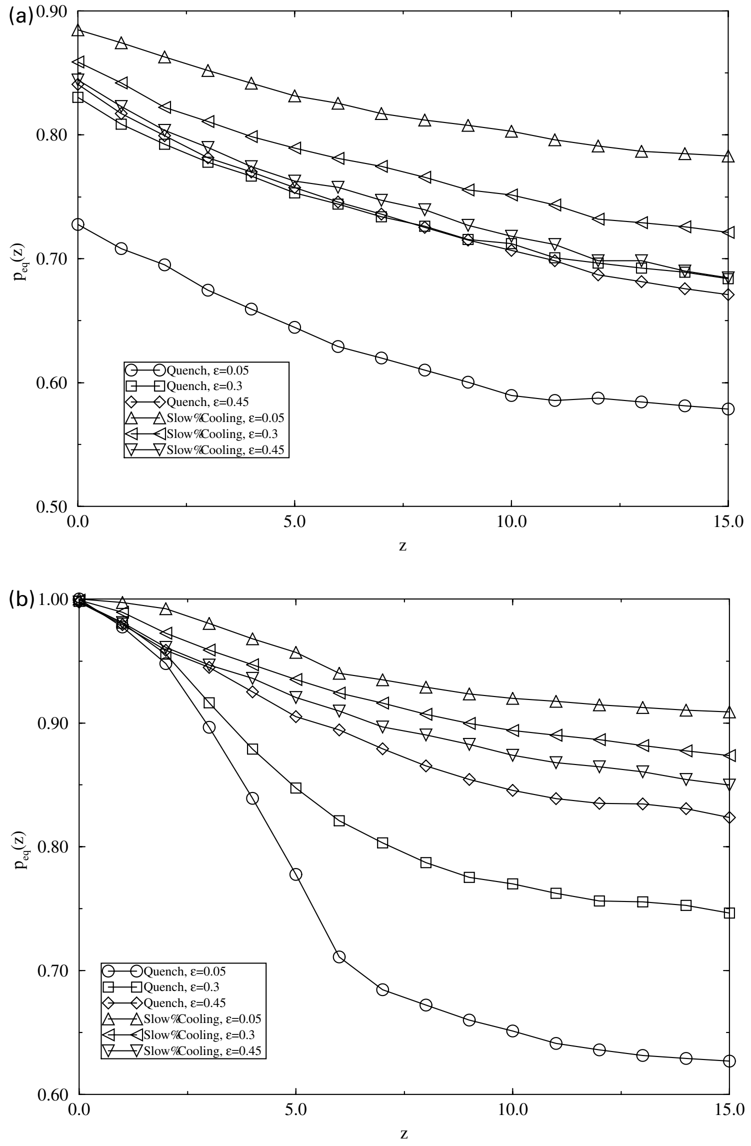

Fig. 8. The late-time domain overlap function after a quench is compared with the equilibrium domain overlap function obtained after a slow cooling of the system. In (a) the strength of the surface interaction is $\sigma = 0.3$ and the width of the surface pattern is $\omega = 18$, while in (b) $\sigma = 1$ and $\omega = 24$.

to avoid such metastable configurations. For a quench at higher temperatures, it becomes much easier for the film to find the ordered state guided by the surface motif.

For stronger surface interactions (Fig. 8b), the film gets perfectly aligned near the substrate whether it is quenched or slow cooled. The magnitude of this ordering decays as one moves away from the substrate. Again, the ordering throughout the film is substantially smaller for the quench case at low temperatures when compared to a slow cooling case at the same final temperature. At higher quench temperatures, the discrepancy is smaller but still persisting. Simulations thus clearly demonstrate the usefulness of slow cooling in achieving a prescribed film morphology guided by a surface pattern.

4. Summary and conclusions

We have presented results from a numerical study of phase separation in thin polymer blend films. Our main emphasis is on the late-time morphology of the films. Due to the lack of an intrinsic characteristic length scale (as in a block copolymer melt, for example), domains of quenched bulk polymer blends grow macroscopically large driven by the interfacial tension. The presence of a substrate potential dramatically alters the growth behavior. We first investigate morphological transitions in a thin film on a flat, homogeneous substrate. In particular, we probe the transition between a completely wetting and a partially wetting surface morphology. This transition is controlled by a competition between surface interactions and the interfacial energy in a thin film. Simulation results show that a stronger surface potential is needed for a thinner film to be in a completely wetting plating morphology.

The competition between the interfacial energy and the substrate potential becomes more pronounced when the blend thin film is cast on a chemically patterned substrate. The energetics of this competition can be understood by comparing the surface potential per strip with the interfacial energy per strip. If the surface interaction is strong enough, the lateral growth of domains is significantly constrained and the domains follow the surface imprints. In order to measure quantitatively the amount of domain overlap with the pre-assigned chemical structure of the substrate as a function of time and the distance from the substrate, we introduce an overlap function. The late-time value of this function after a quench is compared with the overlap after a slow cooling of the film where the system reaches an equilibrium configuration. In addition, we compare film morphology after a quench to the morphology after a slow-cooling case. This helps us to identify possible barriers to reaching equilibrium in experimental situations.

When the surface is patterned with narrow sized strips, a domain line-up with the surface pattern introduces many interfaces. Simulations clearly show that this morphology is not favored by the film when the interfacial energy is larger or comparable to the surface potential. As a result, the late-time patterns cover more than one substrate strips leading to a small overlap with the pattern. A strong surface interaction is able to hold the respective preferred components right on the substrate patterns. But slightly away from the substrate, domain morphology covers many strips by crossing the boundaries set by the substrate patterns. For deep quenches, the amount of overlap is larger when compared to a slow cooling case. This larger overlap after a quench arises from a pinning of the domains near the substrate. This pinning takes place at an early time but can be released at later times by lateral diffusion if the quench temperature is large enough. However, at low temperatures, diffusion is suppressed and the pinning of domains lasts for a long time after a quench. This metastable pinning effect enhances film alignment for the narrow width case. Slow cooling allows the system to spend considerable time at higher temperatures, which clears the local pinning due to the substrate potential.

When the surface pattern width is increased and a strong surface interaction strength is chosen, an almost perfect match between the film morphology and the substrate pattern is observed at the final stages of the evolution process during a quench. However, one needs to consider an intermediate value of the noise strength for this to happen after a quench. If the quench depth is too large, a perfect match is not observed between the overall film morphology and the underlying substrate pattern. The enhanced ordering at higher quench temperatures is due to a reduction of the interfacial tension at higher temperatures and the ability of the system to avoid metastable configurations. Slow cooling improves film alignment at all temperatures, but particularly so at low final temperatures.

Simulations clearly demonstrate that a slow cooling procedure is needed to improve film alignment with the surface motif. Even then one needs to choose the width of the surface pattern judiciously; if the width is too narrow, a perfect alignment will not be obtained even for very strong surface interactions. This is an important guideline for further experimental investigations. Some shortcomings of our simulations should be pointed out in this context. Since our simulations are carried out in two-dimensions, a direct comparison with experiments is not possible. However, we expect that the main findings of the simulations such as the effects of thermal fluctuations and the presence of possible barriers to reach final equilibrium state after a quench are still relevant. Another point to note is the presence of hydrodynamic interactions in experimental situations that is not included in our model simulations. Whether viscous flow would allow for a better film alignment even in a deep quench is an important, unanswered question. Further simulations to address this question is currently underway.

Acknowledgements

An acknowledgment is made to the Donors of the Petroleum Research Fund, administered by the American Chemical Society for support of this work. We thank Dr A. Karim for valuable discussions.

References

[1] Boltau M, Walheim S, Mlynek J, Krausch G, Steiner U. Nature 1998;391:877.

[2] Karim A, Douglas JF, Lee BP, Glotzer SC, Rogers JA, Jackson RJ, Amis EJ, Whitesides GM. Phys Rev E 1998;57:R6273.

[3] Heier J, Kramer EJ, Walheim S, Krausch G. Macromolecules 1997;30:6610.

[4] Rockford LD, Liu Y, Mansky P, Russell TP, Yoon M, Mochrie SGJ. Phys Rev Lett 1999;82:2602.

[5] Boltau M, Walheim S, Schaffer E, Mlynek J, Steiner U. Science 1999;283:520.

[6] Fink Y, Winn JN, Fan S, Chen C, Michel J, Joannopoulos JD, Thomas EL. Science 1998;282:1679.

[7] Jones RAL, Norton LJ, Kramer EJ, Bates FS, Wiltzius P. Phys Rev Lett 1991;66:1326.

[8] Krausch G, Dai C, Kramer EJ, Bates FS. Phys Rev Lett 1993;71:3669.

[9] Wiltzius P, Cumming A. Phys Rev Lett 1991;66:3000.

[10] Shi BQ, Harrison C, Cumming A. Phys Rev Lett 1993;70:206.

[11] Seok C, Freed KF, Szleifer I. J Chem Phys 2000;112:6452.

[12] Kielhorn L, Muthukumar M. J Chem Phys 1999;111:2259.

[13] Gunton JD, San Miguel M, Sahni PS. In: Domb C, Lebowitz JL, editors. Phase transition and critical phenomena, vol. 8. London: Academic, 1983 (see also Bray AJ. Adv Phys 1994; 43:357 for a more recent review).

[14] Krausch G, Kramer EJ, Bates FS, Marko JF, Brown G, Chakrabarti A. Macromolecules 1994;27:6768.

[15] Brown G, Chakrabarti A. Phys Rev A 1992;46:4829.

[16] Krausch G, Dai CA, Kramer EJ, Marko JF, Bates FS. Macromolecules 1993;26:5566.

[17] Chen H, Chakrabarti A. J Chem Phys 1998;108:6897.

[18] Chakrabarti A, Chen H. J Polym Sci Polym Phys 1998;36:3127.

[19] Marko JF. Phys Rev E 1993;48:2861.

[20] Lee BP, Douglas JF, Glotzer SC. Phys Rev E 1999;60:5812.